USGS Award No. 08HQGR0011

A DECISION SUPPORT TOOL FOR OPEN RISK ASSESSMENT SOFTWARE: COLLABORATIVE RESEARCH WITH JOHNS HOPKINS UNIVERSITY AND USGS

FINAL TECHNICAL REPORT

PI: Nichola P. Jones
Co-PI: Judith Mitrani-Reiser
Johns Hopkins University
3400 N. Charles St.
Baltimore, MD 21218
Tel: 410-516-7763
Fax: 410-576-7473
npjones@jhu.edu/jmitrani@jhu.edu
http://www.civil.jhu.edu/

July 2010

Research supported by the U. S. Geological Survey (USGS), Department of Interior, under USGS award number 08HQGR0011. The views and conclusions contained in this document are those of the authors and should not be interpreted as necessarily representing the official policies, either expressed or implied, of the U. S. Government.

Abstract

Extensive damage to woodframe housing during the Loma Prieta and Northridge earthquakes emphasized the vulnerability of this type of structure and strengthened the need to develop methodologies that quantify the risk of woodframe structures in terms of economic measures, life safety, and building operability. There is a current initiative within the USGS to make seismic risk assessment openly available to owners of woodframe houses, which comprise the largest population of buildings exposed to seismic hazard. This initiative is working towards an interactive web-based tool, known as ResRisk-WH (Residential Risk – Woodframe Houses), that queries homeowners for basic descriptions of their homes (e.g., location, size, age, etc.) for use in a subsequent automated risk analysis. The purpose of this project was to develop tools to package into ResRisk-WH that would allow owners to assess the vulnerability of their homes in terms of various performance metrics, and to assess the impact of using simplified structural models that improve the software's running time without compromising accuracy.

The performance-based earthquake engineering (PBEE) methodology used to calculate the performance metrics of interest includes: a hazard analysis, structural analysis, damage analysis, and a loss analysis. The loss and damage analysis procedure can be computationally expensive, in which case it is difficult to incorporate into an interactive risk assessment web-tool. This project explores a simplified analytical methodology for PBEE, including an optimized selection of engineering demand parameters that will enhance the usability of ResRisk-WH. This project explores the effect these simplifications have on the risk assessment results by comparing them with the results of a more detailed PBEE analysis for two baseline wood-frame structures. We ultimately provide recommendations for structural model simplifications that can be taken while giving a reasonably small error in the loss results.

An essential component of the PBEE analysis process is to quantify the seismic performance of woodframe housing in terms of building safety (i.e., probabilities of red tagging). This project demonstrates how the probability of building safety can be estimated through a "virtual inspector" using the probabilities of damage of the building's components and applying current building inspection guidelines. An analytical model, otherwise known as the *virtual inspector* is used to estimate the probabilities that the building will be tagged at various levels of ground

shaking with the well-known red, yellow, and green safety placards, based on current U.S. guidelines. This model may also be used to locate the areas of higher probability of damage in the structure. The *virtual inspector* probabilistically estimates building safety by matching up the damage descriptions from the fragility functions of the structural and nonstructural components with the damage descriptions from inspection guidelines.

1 INTRODUCTION

Quantitative risk assessments are seldom carried out for wood-frame houses because the process is expensive, and because the tools to perform such an assessment have been lacking. The United States Geological Survey (USGS) develops and makes publicly available seismic hazard maps that display levels of ground shaking for various probability levels. These maps, updated earlier this year for the lower 48 states (Peterson et al., 2008), are used in seismic design provisions, in setting insurance rates, and for seismic loss studies. The USGS is in a unique position to extend the National Seismic Hazard Maps and develop new risk assessment tools. The USGS has thus undertaken the important role of developing a risk assessment tool that can be used to assess the performance of wood-frame houses, which make up the majority of the residential building stock in the U.S.

ResRisk-WH is to be a publicly available web-based tool that computes the seismic risk of individual wood-frame houses given basic input provided by homeowners. This tool computes the seismic risk on residences via the following steps: (1) determine the earthquake hazard curve from the USGS National Seismic Hazard Maps using the specific location of the building and estimates of the soil conditions there; (2) prepare a simplified structural model of the building using either archetypical or user-specified floor plans specified by the homeowner, construction information about the property that the average homeowner can provide (e.g., house age, square footage, number of stories, foundation types, and wall finishes), and library-defined values for structural model parameters based on the information provided by the user; (3) select ground shaking time histories—representative of the potential earthquakes that dominate the seismic hazard at the location of the house—to use as input for the computer model of the house; (4) stochastically simulate the earthquake damage and perform a safety evaluation of the house based on the structural analysis results and pre-defined fragility curves for structural and nonstructural components typically found in wood-frame construction; and (5) estimate resulting losses for the home using cost distribution functions representative of the repair effort needed to return the simulated damage back to an undamaged state.

After the Northridge earthquake, 9,264 or 12% of the wood frame buildings in Los Angeles, Ventura, and Orange Counties were either yellow- or red-tagged by building inspectors (EERI, 1996a). In Los Angeles County alone, 56,000 residential units (a majority of which are wood frame) were tagged red or yellow forcing a significant number of people to vacate their homes (EERI 1996b). Damage statistics like these warrants the need to model building performance in terms of safety tagging and to estimate the probability of red-tagging of buildings in future seismic events. This project integrates the *virtual inspector* developed by co-PI Mitrani-Reiser (2007) into the ResRisk-WH platform to estimate the probability of red-tagging of detached single-family dwellings given the home's location and design. The framework of the *virtual inspector* is adopted to probabilistically estimate building safety by matching up the damage descriptions from the fragility functions of the structural and nonstructural components with the damage descriptions from inspection guidelines.

The interactive functionality of this risk assessment web tool demands that the structural analysis and subsequent loss analysis be carried out in a small amount of time. However, nonlinear dynamic analyses of structures can be computationally expensive and are the limiting factor for the 'on-the-fly' loss estimation needed for ResRisk-WH. This project also explores the feasibility of using simplified models for two archetypical buildings, and the effects that these simplifications ultimately have on the loss results. These results are compared with previous work on these archetypical buildings (shown in Figure 1) from the CUREE-Caltech Woodframe Project.

Figure 1. Front and rear elevations for (a) the small house index building, and (b) the large house index buildings (Porter et al., 2002).

2 BUILDING MODELS

The index buildings were modeled in the CUREE-Caltech Woodframe Project and in this study using RUAUMOKO, a nonlinear dynamic analysis computer program developed for earthquake engineering applications (Carr, 2000). An example of the original CUREE model for the *small house* is given in Figure 2; this model, representing a typical one-story, single-family home (1200 ft^2 sf) built in the 1950s, uses a planar "pancake" system with the floor diaphragm and the roof diaphragm superimposed on top of each other (Isoda et al., 2001). The foundation of the building is connected to the first floor using two zero-length nonlinear shear springs in each direction, representing the cripple walls of the house. The first floor diaphragm is connected to the roof diaphragm using seven zero-length nonlinear springs in each direction (two for the exterior walls sheathed with stucco, two for the gypsum wallboard sheathing on the inside of the exterior walls, and three for the interior walls sheathed with gypsum wallboard). These zero-length nonlinear springs for the shear walls were modeled to follow the Wayne Stewart hysteresis rule (Stewart 1987) that incorporates stiffness and strength degradations. Finally, frame elements are used along the edge of the diaphragms to connect the quadrilateral finite elements to the nonlinear spring members. The floor and roof diaphragms were modeled using linear-elastic quadrilateral finite elements. The weight of the building is computed by adding the dead load of its structural and nonstructural components, and is distributed as lumped seismic weights at the nodes of the quadrilateral elements according to their tributary areas. Similar pancake models are used for the *large house*, which is a typical two-story, single-family home (2420 ft^2 sf) built in the late 1980s or early 1990s. These models are taken from the

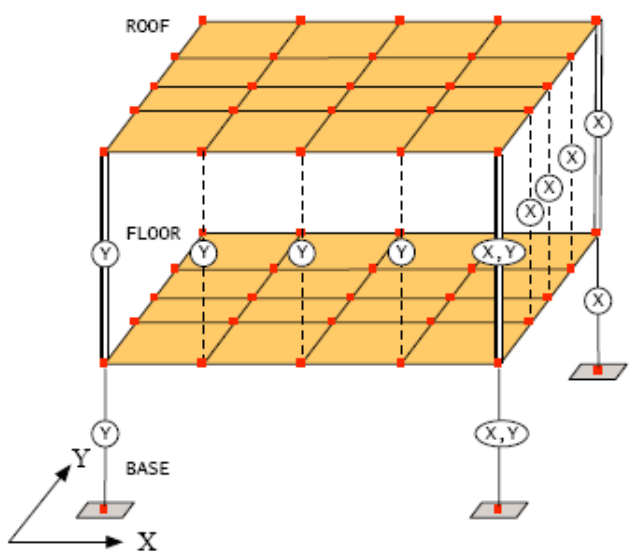

Figure 2 Structural model of the small house index building, where the x-axis is parallel to the long side of the house and the y-axis is parallel to the short side of the house. The solid vertical lines of the original model, used in the CUREE-Caltech Woodframe Project (Isoda et al., 2001), depict the spring elements that represent the exterior walls of the house, and the dashed vertical lines are representative of the interior walls. Encircled 'x' and 'y' letters depict the direction of the planar spring elements (walls).

CUREE-Caltech project where springs were added to account for the OSB (oriented strand board sheathing) used on the exterior walls; instead of using frame elements, displacements of the nodes in the *large house* of the quadrilateral elements are constrained to be equal to the displacements of the nodes connecting these to the shear wall elements.

The original CUREE model for the *small house* index building is made up of 53 nodes, 130 elements (including diaphragm, frame, and spring elements), and uses 20 types of materials; the *large house* index building model is made up of 97 nodes, 108 elements, and 50 types of materials. The computation time for one analysis of the *small house*, using an ordinary desktop computer, takes almost 11 seconds. Although the time for each structural analysis may appear modest, a typical probabilistic risk analysis application in ResRisk-WH can require several hundreds of these simulations. Therefore, without further simplifications this approach is too computationally demanding to be practical for an interactive web-based tool. It is, thus, our goal to streamline the structural analysis without degrading the original model (i.e., without significantly changing the risk analysis results).

Two strategies for simplification are devised for the small and large house index buildings. The first simplification strategy (*S1*) models each diaphragm as a single linear-elastic quadrilateral finite element, and lumps the spring elements of the same wall type (i.e., the same material properties) in each direction to spring elements located at the corners of diaphragm based on force and moment equilibrium (e.g., the five shear spring elements representing gypsum wallboard on the interior and exterior walls in each direction of the small house are lumped into two springs at the corner nodes).

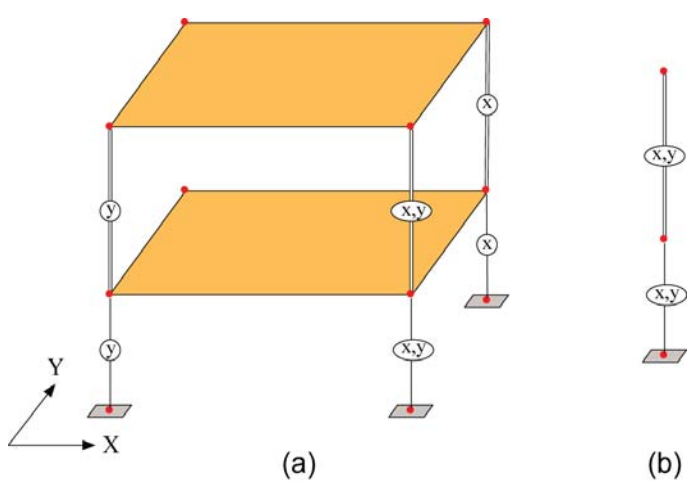

Figure 3 Simplified structural models of the small house index building. (a) The simplified S1 model uses single quadrilateral elements to model the floor and roof diaphragms and lumps the spring elements of the exterior and interior walls at the corners of the diaphragm. (b) The simplified S2 model replaces the diaphragms with point nodes and lumps all spring elements of the same type in each direction.

The layers, nodes, and elements for the *S1* model of the small house are depicted in Figure 3 (a). The second, more drastic simplification strategy (*S2*), shown in Figure 3 (b), replaces the diaphragms with point nodes and lumps the spring elements of the same wall type in each direction into a single spring. Therefore, *S2* has one spring (representing the cripple walls) in each direction between the base and the floor, and has two springs (representing the stucco walls and gypsum walls) in each direction between the floor and the roof. The number of nodes, elements, materials, and natural frequencies for the original, *S1*, and *S2* models of the small house and of the large house, as well as the computation times for the structural analysis are summarized in

Table 1.

Table 1. Details of the original and simplified structural models used for the small and large houses, along with their dynamic characteristics and computation time per structural analysis.

		Small House			Large House		
		Original	**S1**	**S2**	**Original**	**S1**	**S2**
Structural Model	Nodes	53	11	3	97	11	3
	Elements	120	14	6	108	26	12
	Materials	20	12	6	50	26	12
	Comp. Time	10.93s	1.65s	0.47s	9.40s	1.69s	0.84s
Natural Period (sec)	Mode 1	0.19 (Y)	0.19 (Y)	0.19 (Y)	0.17 (Y)	0.17 (Y)	0.13 (X)
	Mode 2	0.17 (X)	0.18 (Y)	0.17 (X)	0.14 (X)	0.14 (X)	0.13 (Y)
	Mode 3	0.14 (Y)	0.17 (X)	0.05 (Y)	0.09 (Y)	0.12 (Y)	0.06 (Y)
	Mode 4	0.08 (Y)	0.08 (X)	0.05 (X)	0.06 (Y)	0.06(Y)	0.06 (X)
	Mode 5	0.08 (X)	0.05 (Y)		0.06 (Y)	0.06 (Y)	

3 GROUND MOTION SELECTION AND STRUCTURAL ANALYSIS

A complete risk analysis of a building requires an estimation of the building performance in terms of engineering demand parameters (*EDP*), for a wide range of seismic hazard intensity levels. The seismic intensity measure (*IM*) used in this study is the 5%-damped elastic spectral acceleration at the building's first mode period, $S_a(T_1)$. Twenty seismic intensity levels are considered, ranging between $S_a(T_1)$=0.1g to 2.0g, with a step size equal to 0.1g. The ground motions selected for the CUREE-Caltech Woodframe Project, which were originally developed for Los Angeles as part of Phase 2 of the SAC Steel Project (Somerville et al., 1997), are used in the present study. Each of these recordings is scaled to match each target spectral value and is,

subsequently used as input for the structural models described above. The scaling of the ground motions is consistent for all models of the small house and large houses, including the original and simplified models. We maintain the same scaling factors of the ground motions so that we could compare the damage and loss results of models excited with the same input ground motions. Note that there is less than a 2% difference in $S_a(T_1)$ between the original and the simplified models for the small house and its corresponding *S1* and *S2* models and for the large house and its corresponding *S1* model; there is a 20% decrease in the natural period in the *S2* model of the large house. The ground motions and scaling factors used with the small and large houses can be found in the Tables 4-4 and 4-5 of the CUREE-Caltech Woodframe Project report (Porter et al., 2002), respectively, except that a few of the scaling factors are corrected with respect to the values in those tables.

Nonlinear dynamic analyses are performed for the two index buildings using the scaled ground motions for each of the twenty levels of ground shaking intensity. The same number of ground motion time histories selected by Porter et al. (2002) are used for each hazard intensity level—17 to 20. Each ground motion record includes two horizontal time histories for use in the structural analysis. For the non-collapse[1] simulations, the structural analysis results plotted in Figure 4 and Figure 5 show the mean story drift ratio for each *IM* level. The individual story drift ratios are averages over all the peak wall drift ratios (wall drifts normalized by wall heights) in a story and for each direction. The solid black lines with circle markers are the mean drift values of the original small and large house models (same as CUREE-Caltech models) across the twenty hazard intensity levels considered in this study; the grey shaded area indicates +/- one standard error of the mean (SEM). The results for the simplified models, *S1* and *S2*, are shown by the dashed lines with green solid triangle and red asterisk markers, respectively.

The mean story drift values of the lowest wall level are larger than those of the upper stories for the small index building because the weight of the building associated with the upper stories is small as compared to the lower level and because the upper stories are stiffer than the lower stories. The upper story of the small house is more than four times stiffer in the x-direction than the lower level; the upper story of the small house is five times stiffer in the y-direction than the

[1] A collapse simulation is one where any peak story drift ratio is equal to or greater than one.

lower story. Note that the y-axes in Figure 4 are scaled by 10^{-4} for the upper stories, and that the difference in drift values between the upper and lower stories is almost three orders of magnitude. The simplified models capture the behavior of the small house fairly well except at a few intensity levels. The most noticeable difference occurs at Sa_{T1} = 1.5g, where the mean drift ratios of the cripple walls of the small house are overestimated (30-35% error) by the simplified models. The simplified models do not capture a "collapsed" damage state for two of the ground motions at this intensity level and are thus included in mean structural response plots; the deformations are large in the simplified models for these two ground motions, which results in a larger mean drift ratio of the cripple walls and thus the apparent spike in the plot.

The mean story drift values of the lowest wall level of the large house index building are also larger than those of the upper story because the weight of the building associated with the upper stories is small as compared to the lower level; the stiffness of the upper story of the large house is 28% stiffer in the x-direction and comparable in stiffness to the lower story in the y-direction. The simplified models capture the behavior of the large house well in the x-direction, but consistently underestimate the behavior of the first story, overestimate the behavior of the second story, and fall outside the SEM. The *S1* model underestimates the first-story mean drift ratio values in the y-direction by up to 32%, and overestimates the second-story mean drift ratios by no more than 30%; the *S2* model underestimates the first-story mean drift ratio values in the y-direction by no more than 48%, and overestimates the second-story mean drift values by up to 60%. The simplified models do not capture the torsional behavior of the original model well and thus, contributes to the inconsistency in the mean IDR results for the large house.

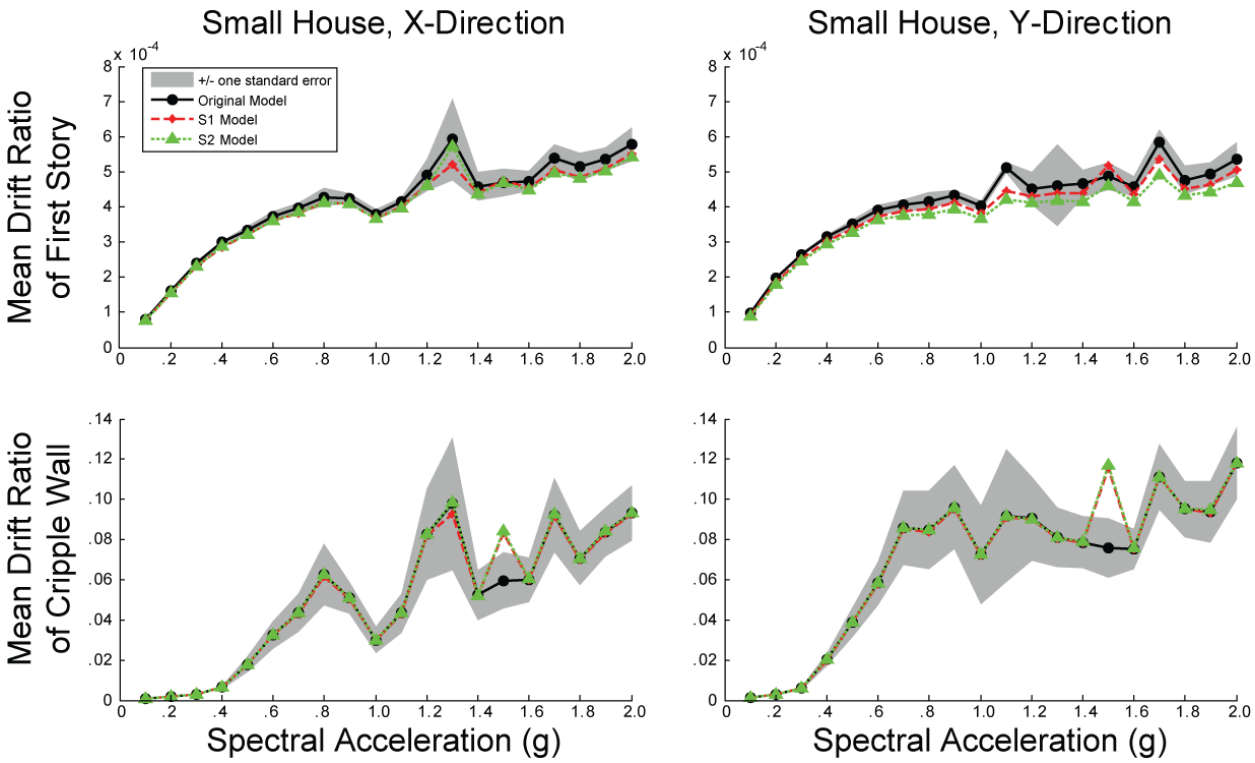

Figure 4. Mean story drift ratios for *small house* index building in x- and y-directions.

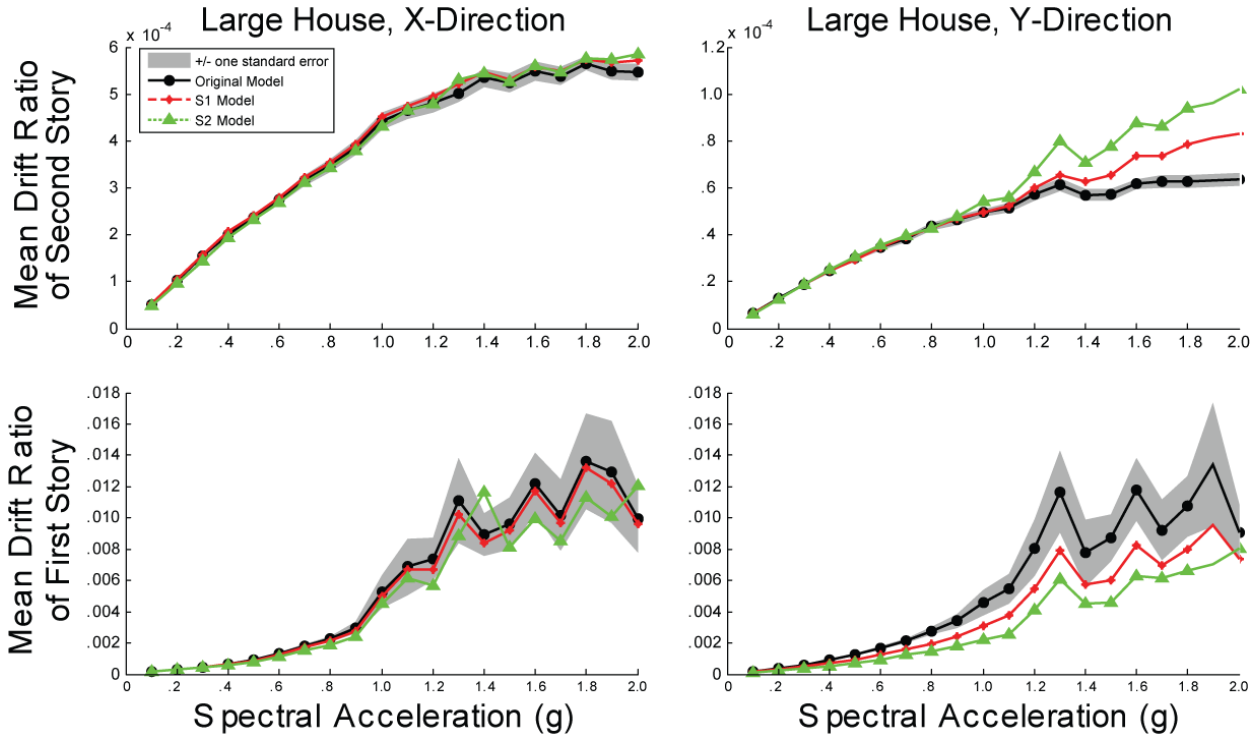

Figure 5. Mean story drift ratios for *large house* index building in x- and y-directions.

4 DAMAGE ASSESSMENT

The results from the structural analyses described in the previous section are then used to simulate the earthquake damage of the index buildings. The first step of the damage analysis procedure is to create a detailed list of damageable structural and nonstructural building components, which is populated from architectural and structural drawings. Those components considered safety critical in the small and large house index buildings are considered for the damage and safety assessments in this study. The safety assessment of the *small house* depends on the following damageable components: cripple walls, exterior stucco walls, and interior gypsum wallboard partitions. The damageable components considered for the safety assessment of the *large house* include: exterior and interior shear walls, and the interior gypsum wallboard partitions. Note that the types of damageable components included in these analyses are constrained by the number engineering demand parameters that can be assessed using the simplified models. For example, peak floor accelerations would need to be calculated by the structural model to determine the probability of damage of some nonstructural components, such as water heaters.

Fragility functions are needed to translate the structural analysis results into damage states. For a given value of *EDP* of a building component, the fragility functions give the probabilities of being in or exceeding the prescribed damages states. Fragility functions are cumulative distribution functions of damage that are created using experimental data, analytical investigation, expert opinion, or some combination of these. Lognormal probability distributions are commonly used in the loss estimation literature (e.g., Beck et al., 2002; Aslani and Miranda 2004; Goulet et al., 2007) to quantify the fragility corresponding to the various damage states for each damageable structural and nonstructural component. To fully describe a lognormal distribution, the median and logarithmic standard deviations are needed. Therefore, the median capacity and logarithmic standard deviation of capacity (defined in terms of the *EDP* value that causes a component to reach or exceed a given damage state) are used to create the fragility functions, and then to estimate damage. The lognormal distribution parameters describing the fragilities for all the damageable components are given in Porter et al. (2002).

Simulation (i.e., Monte Carlo Simulation) or analytical procedures (see Goulet et al., 2007) may be used to complete the damage analysis for the building. For MCS, each damageable building component is treated independently and a random number is sampled from a standard uniform distribution to select the damage state for each damageable building component after every realization of the structural analysis. For example, suppose an exterior stucco wall has a 1% drift ratio. Based on the fragility functions of this component type, it has a 27% probability of having no damage (damage state = 0), a 72% probability of cracking stucco (damage state = 1), and a 1% probability of heavy damage to stucco and framing (damage state = 2). If the random number generator gives a value between 0.27 and 0.27+0.71=0.98 (e.g., 0.5), then the wall is in its first damage state, which means it has cracked stucco for the given simulation. Alternatively, the analytical framework for damage estimation, shown mathematically in

$$P[DM_{ij} \mid NC, im] = \int_{edp_i} P[DM_{ij} \mid edp_i] p(edp_i \mid NC, im) dedp_i \quad (1)$$

where $P[DM_{ij}|NC, im]$ is the probability of reaching or exceeding the damage state *j* for a given building component *i,* conditioned on the structure not collapsing (*NC*) and on a given hazard intensity (*IM*) level; $P[DM_{ij} \mid edp_i]$ is the probability of reaching or exceeding the damage state *j* for a given building component *i* and conditioned on EDP_i associated with the component of type (this probability comes directly from the corresponding fragility function); $p(edp_i \mid NC, im)$ is the probability density of EDP_i, conditioned on the structure not collapsing (*NC*) and on a given hazard intensity (*IM*) level. In order to evaluate the probability density function of edp, a lognormal distribution is fit to the structural response data, as is done in damage assessments of other types of structures (e.g., Haselton et al., 2007; Aslani and Miranda 2004). Additionally, equation (1) assumes that each assembly group is composed of damageable components sensitive to the same *EDP*, and that their damage states are modeled as perfectly correlated and conditionally independent, given *EDP*, from all other assembly groups.

Damage results for structural models

The ResRisk-WH platform employs MCS for the damage assessment, which was used for a damage assessment of the two example buildings. The average (mean) damage results of the most vulnerable and safety-critical components of the small and large houses are given in Figure 6 and Figure 7. The probability of having heavy damage and collapse of the cripple walls in the

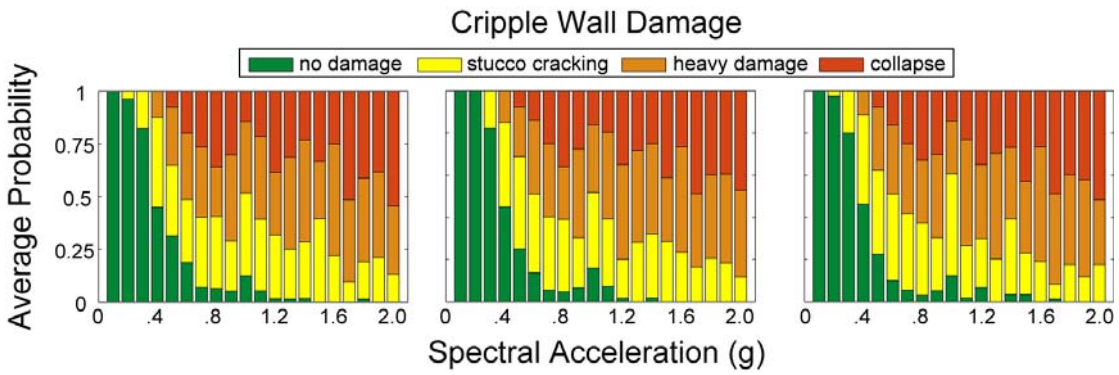

Figure 6. Average probabilities of damage of the cripple walls in the small house for (from left to right) the original, the S1, and the S2 models.

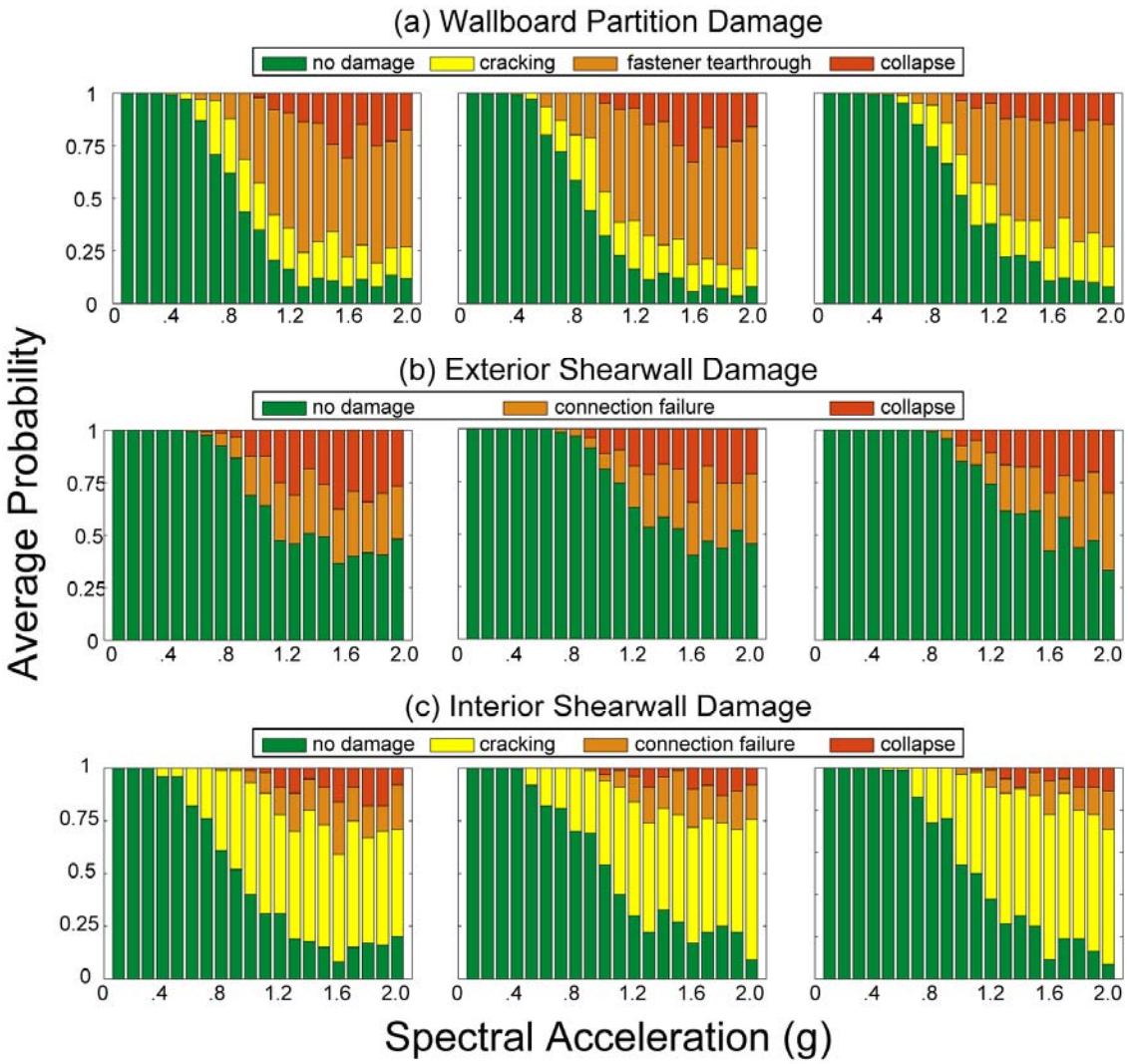

Figure 7. Average probabilities of damage of (a) the gypsum wallboard partitions in the first story of the large house, (b) the exterior shearwalls in the first story of the large house, and (c) the interior shearwalls in the first story of the large house.

small house (Figure 6) at Sa = 0.5g is 35% for the original model, 31% for the S1 model, and 38% for the S2 model; it is ≥50% for all hazards levels after this point for all the models except at Sa = 0.5g. Although the probability of having heavy damage and collapse of the cripple walls monotonically increases with increasing Sa values, it drops around Sa = 1.0g corresponding to the dip in structural response of the cripple walls (Figure 4) at this intensity level. This figure depicts the historically-known vulnerability of unbraced cripple walls caused by their inability to transfer loads to the foundations of dwellings.

Figure 7 (a)-(c) show the average probability of damage of first-story walls in the *large house*. These plots show that the nonstructural components (wallboard partitions in (a)) reach higher levels of damage (i.e., fastener breakthrough and collapse) earlier than structural components (shearwalls in (b) and (c)) in the same story. Although gypsum wallboard partitions are not safety critical, they are significant contributors to economic losses, accounting for roughly 25% of total repair costs (Porter et al., 2002). These results suggest that damage to the wallboard partitions in woodframe housing is a substantial driver for seismic loss as they are for reinforced concrete commercial buildings (Mitrani-Reiser and Beck 2007). The *S2* model underestimates the damage of the wallboard partitions as well as the interior shearwalls.

5 LOSS ASSESSMENT

The cost to repair each damaged component back to an undamaged state is estimated using the damage analysis results and repair-cost distribution functions. These repair costs distribution functions are typically created using empirical loss results from historical events and/or advice from professional cost estimators. The cost distribution functions used in this study were developed based on the guidance of a professional cost estimator and are given for all components of the small and large houses in the CUREE-Caltech report (Porter et al., 2002). Like the fragility functions, lognormal probability distributions are found to appropriately capture the uncertainty in unit repair costs. The cost to repair the damaged building components of each simulation is estimated using Monte Carlo procedures, similar to the steps taken in the damage analysis. A random sample is taken from the lognormal distribution of the unit repair cost for a building component type in a given damage state, by transforming a random sample from a standard normal distribution. This unit repair cost is then multiplied by the number of

units in the given damage state to get a total loss per type of damageable component. The repair cost of a collapsed house is equal to its replacement cost. Note that a collapse is reached when there is lateral displacement without bound, when any peak story drift ratio is equal to or greater than one. The total repair cost, or total loss, is calculated by summing the repair cost over all damageable components in the building, for each simulation; a plot of the mean loss across simulations for each in a range of *IM* values is known as a vulnerability curve. The vulnerability curves for all three models of the small and large houses are given in Figure 8.

Loss results for simplified structural models of the Small House

The losses for the small house are given in the top half of Figure 8, where the mean total loss of the *original* model is plotted (as the Damage Factor, DF, which is equal to mean total loss divided by total replacement cost) in the solid black line with solid circle markers, and the grey shading indicates +/- one SEM. The loss results for the simplified models, *S1* and *S2*, are depicted using dashed lines with green triangle and red asterisk markers, respectively. The damage to the flexible cripple walls dominates the repair costs for the non-collapsed simulations, as well as for some of the collapsed cases. The cost associated with repair/replacement for collapsed cases begins to control the mean total loss for intensity levels above $S_a(T_1)$ = 0.7g. After this intensity measure, the losses oscillate between DF = 0.15 and 0.24, and the dispersion (in Figure 8) of the total repair cost increases substantially. It is important to note that the increase in the variance of the total loss is not due to the uncertainty of the repair costs for individual components, nor to the uncertainty of the repair cost associated with collapse. Instead, this increase is due to a growing number of collapsed cases for increasing intensity levels, and the significant gap that exists between the total repair costs associated with collapsed and non-collapsed cases. The original model of the small house gives probabilities of collapse that fluctuate between 45% and 65% for Sa ≥ 0.7g, and reaches the maximum of 72% probability of collapse at the largest intensity level; the simplified models follow a similar trend with calculated probabilities of collapse. The shape of the vulnerability curves, thus, mimics the curves of probability of collapse. Since the simplified models capture building collapse and the behavior of the cripple walls fairly well, the loss results estimated from the simplified models fall within the SEM of the original *small house* model, and have no more than 20% error. Note that these results are sensitive to the definition of building collapse since it is a driver for the losses at large IM's.

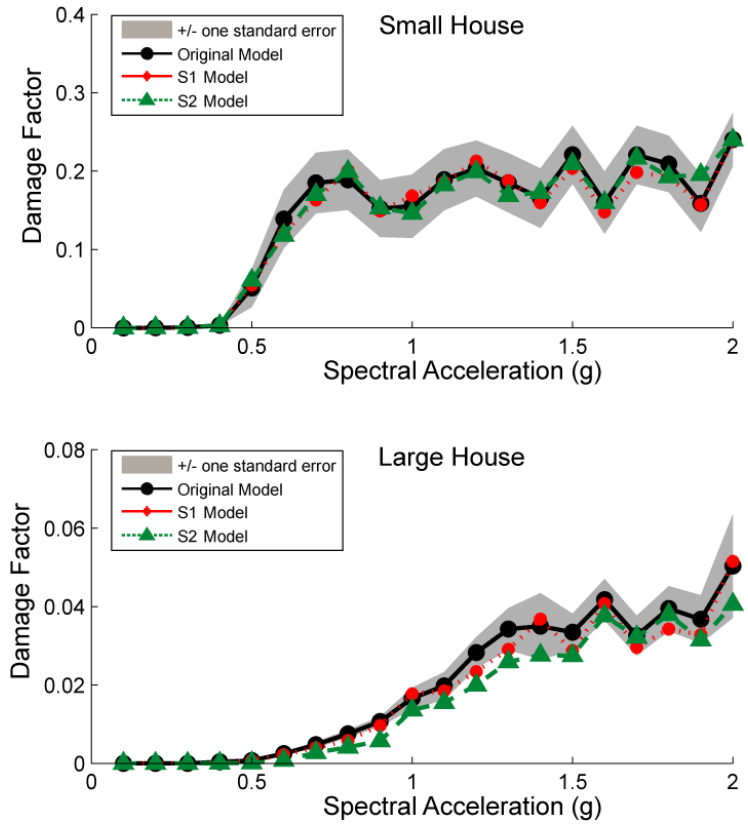

Figure 8. Vulnerability curves for small and large houses.

Results for the simplified structural models of the Large House

The losses for the large house are given in the bottom half of Figure 8. Again, the mean total loss of the *original* model is plotted with a solid line, the simplified models are plotted with dashed lines, and the grey shading indicates +/- one SEM. Unlike the small house, the large house has very few simulations (3 for the original and S1 model, and none for the S2 model) that result in a collapsed state. For the non-collapsed cases, the repair costs of the large house are governed by damage to the interior and exterior walls in the first story. The losses for all models of the large house increase monotonically for intensity levels up to $S_a(T_1)$ = 1.3g, after which point they begin to oscillate similar to the losses of the small house. The losses for model *S1* closely follow the loss trend of the original model, fall within the SEM of the original model, and have no more than a 17% error. The *S2* model consistently underestimates the losses of the original model and gives up to a 30% error; this simplified model does not capture the behavior of the interior shear walls of the original model nor does it result in collapsed cases, as the original and *S1* models do.

6 SAFETY ASSESSMENT: THE VIRTUAL INSPECTOR FRAMEWORK

The inspection of buildings and other structures after a seismic event helps to identify damage that may be life threatening to people, and to locate buildings that have collapsed or are in imminent danger of collapse. The performance assessment procedure in ResRisk-WH gives a

complete description of the building damage for each structural analysis run given a seismic loading. The damage descriptions resulting from this analysis are mapped to safety assessment guidelines to establish the probability of red-tagging of a structure for a specified range of hazard levels.

The Applied Technology Council's *Procedures for Postearthquake Safety Evaluation of Buildings* document (ATC 20 1989; ATC 20-2 1995; ATC 20-3 1996) was written to provide clear guidelines for post-earthquake building evaluation using a three-level evaluation methodology: rapid evaluation (emphasis is on exterior of building), detailed evaluation (thorough examination of interior and exterior), and engineering evaluation (recommended when visual inspections are not sufficient to determine damage to building). The outcome of these evaluations is to tag the buildings with red, yellow, or green placards that designate a building as unsafe, restricted for use, or apparently safe, respectively.

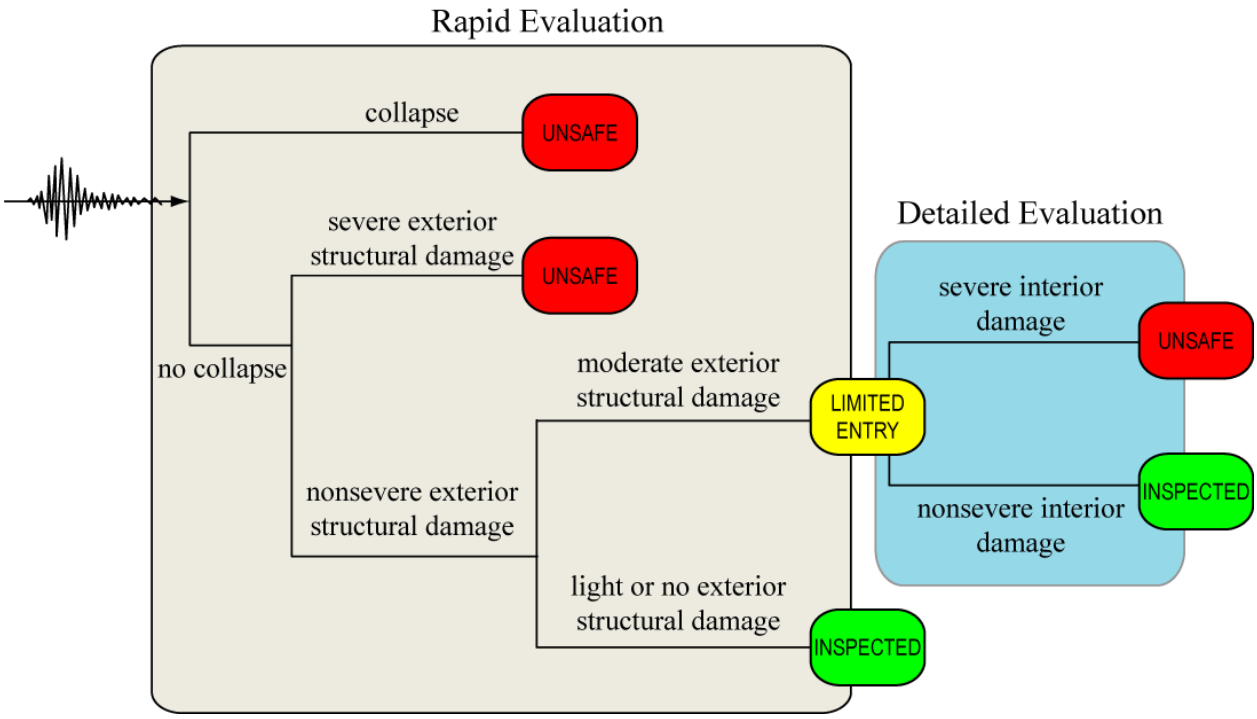

Figure 9 Event-tree diagram depicting the framework of the virtual inspector to estimate the probability of safety tagging of building given a seismic event or hazard level of interest (from Mitrani-Reiser 2007).

These ATC-20 guidelines were used by Mitrani-Reiser (2007) to create a *virtual inspector* or a computer model that probabilistically estimates building safety using damage analysis results similar to those produced by ResRisk-WH. The basic structure for this virtual inspector is given in the form of an event tree and is shown in Figure 1. The first block of the methodology, (a), corresponds to ATC-20's rapid evaluation, which evaluates the structural integrity of a building and the probability of a red, yellow or a green tag being posted, based on what would be a speedy inspection of the exterior structural components. The second block, (b), relates to ATC-20's detailed evaluation and includes a more thorough inspection of the structural components in the exterior as well as the safety critical components in the interior of the building.

The first branch of the event tree in Figure 9 determines the probability of a building's red tagging due to severe leaning and/or collapse (global or local) of the structure. The complement of this branch is for the event where the building does not collapse in any way nor is seriously out of plumb; this branch breaks off into three others that classify the overall damage to the exterior structural members as "severe," "moderate," and "none or light." The structural analysis is used to determine the probability of building collapse and to determine the probability of damage of the structural elements, which are then used to determine the probabilities of a building being red, yellow and green tagged, given an intensity measure and completion of a rapid evaluation. These probabilities are given in Equation 1, where TAG_R, TAG_Y, TAG_G correspond to red, yellow and green tags, respectively; RE denotes rapid evaluation; $P[C|im]$ is the probability of collapse given an intensity measure; $P[NC|im]$, the probability of no building collapse, is equal to $1 - P[C|im]$; and $P[\text{severe ext. struct. damage}|im]$, $P[\text{moderate ext. struct. damage}|im]$, $P[\text{light or no ext. struct. damage}|im]$ are the probabilities of severe, moderate, and light or no damage, respectively, to the exterior structural members given that the building has not collapsed.

$$\begin{aligned} P[TAG_R \mid im, RE] &= P[C \mid im] \\ &\quad + P[\text{severe ext. struct. damage} \mid im, NC]P[NC \mid im] \\ P[TAG_Y \mid im, RE] &= P[\text{mod. ext. struct. damage} \mid im, NC]P[NC \mid im] \\ P[TAG_G \mid im, RE] &= P[\text{light/no ext. struct. damage} \mid im, NC]P[NC \mid im] \end{aligned} \tag{2}$$

If the tagging of a building is not determined to be red or green after the rapid evaluation, a detailed evaluation is typically recommended by building inspectors. The detailed evaluation procedure, in Figure 9, follows the rapid evaluation's yellow tagging. The "virtual inspector" diverges from the ATC-20 guidelines in one respect for the detailed evaluation. In reality, the detailed evaluation of a building that has been yellow tagged can result again in a yellow tag if the inspector feels that a specific area in or near the building is unsafe or if the visual inspection of the structure is not sufficient to estimate the degree of damage to the building. Some examples of an area considered unsafe, and thus yellow-tagged are: a canopy that has collapsed over an entrance; possible falling hazards from damaged veneers or chimneys; and severe damage to nonstructural components such as ceilings and light fixtures. These components are either not present or not considered in the current damage analysis of the index buildings. Additionally, if visual inspection is limited during a seismic safety field inspection, the inspector would then recommend that the owner contract a structural engineer to conduct the engineering evaluation. However, the nonlinear dynamic structural analysis and the damage analysis described of ResRisk-WH offer information similar to that of the engineering evaluation. For this reason, the detailed evaluation of the *virtual inspector* is assumed to terminate with a red or a green tag. The probabilities of a building being red and green tagged, given an intensity measure and the completion of a detailed evaluation are:

$$
\begin{aligned}
&P[TAG_R \mid im, DE] = P[\text{severe int. struct. damage} \mid im, NC]P[NC \mid im], \\
&P[TAG_G \mid im, DE] = P[\text{nonsevere int. struct. damage} \mid im, NC]P[NC \mid im], \\
&P[DE \mid im, RE] = P[TAG_Y \mid im, RE],
\end{aligned}
\tag{3}
$$

where *DE* denotes detailed evaluation; and *P*[severe int. struct. damage|*im, NC*], *P*[nonsevere int. struct. damage|*im, NC*] are the probabilities of severe and nonsevere (i.e., none, light, or moderate) interior structural damage, respectively, given that the building has not collapsed and for a given intensity measure. Note that *any* structural member (exterior or interior) in the severe damage state is considered to produce a red tag, and *any* exterior structural member in the moderate damage state produces a yellow tag. The probability of the benchmark building being red tagged and green tagged is computed from:

$$P[TAG_R \mid im] = P[TAG_R \mid im, RE] + P[TAG_R \mid im, DE]P[DE \mid im, RE],$$

$$P[TAG_G \mid im] = P[TAG_G \mid im, RE] + P[TAG_G \mid im, DE]P[DE \mid im, RE]. \quad (4)$$

7 SAFETY ASSESSMENT RESULTS

The results from the damage analyses described in the previous section are then used to simulate the post-earthquake safety tagging of the index buildings. The power of the virtual inspector depends on the level of detail in the structural and damage analyses. The first step in the inspection procedure is to determine if there is lateral displacement without bounds (or global collapse). Each structural analysis simulation terminates in a "collapsed" or "non-collapsed" damage state. A simulation resulting in collapse is defined as one where the numerical algorithm does not converge or where the resulting structural response is not physically feasible (e.g., *IDR* ≥ 100%). Those simulations that collapse are summed per intensity measure to calculate $P[C \mid im]$, and warrant a red tag according to ATC-20's checklist for safety evaluation of a structure during a rapid evaluation (ATC 20-3, 1996). The damage analysis of the pancake-model results are used to estimate the probability of tagging in the event that there is no global collapse of the building (all other branches of the event tree in Figure 1). The probability of the benchmark building being posted with a red and green tag is calculated using Equation (4).

The methodology for virtual building-safety tagging presented here attempts to closely mimic the post-seismic conditions encountered by building inspectors. The unbraced cripple walls of the *small house* index building are the components that would raise flags of concern with the inspectors who are assessing the structure. If any cripple wall is in a 'collapsed' damage state (median of IDR, x_m = 8.3% and the logarithmic standard deviation of IDR, β = 0.1), that given simulation will result in a red tag. If none of the cripple walls are in a 'collapsed' damage state, but if any of the exterior walls have 'heavy' damage to their framing and stucco (median of IDR, x_m = 3.1% and the logarithmic standard deviation of IDR, β = 0.47), and the interior walls are in their collapsed damage state (median of IDR, x_m = 1.6% and the logarithmic standard deviation of IDR, β = 0.2), then the simulation will also result in a red tag. If there is no collapse of the cripple walls and no heavy damage of the exterior walls, then the simulation will result in a green

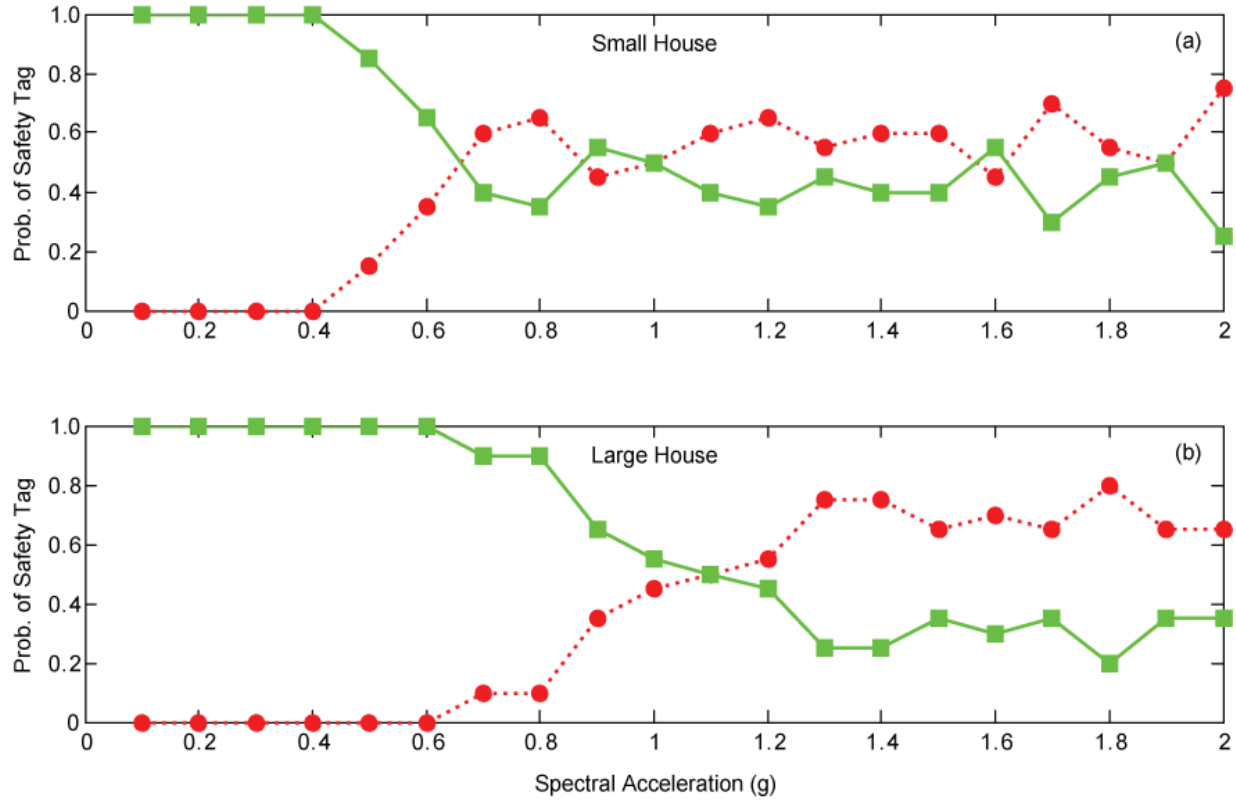

Figure 10 A comparison of the probabilities of building safety tagging for the (a) small house, and (b) large house; the color of the lines correspond to ATC-20's red ("UNSAFE") and green ("INSPECTED") tags.

tag. The number of simulations resulting in red and green tags are then added and normalized by the total number of simulations (that are not globally collapsed) per intensity measure to calculate the probability of the typical *small house* being red-tagged given *NC* and for a given ground motion intensity level.

The safety assessment results for the *small house* are given in Figure 10(a). This plot demonstrates that the *small house* has a near-zero probability of receiving a red tag resulting from a detailed evaluation for earthquakes with hazard levels less than or equal to S_a =0.4g. The probability of the small house receiving a red tag increases linearly until S_a =0.7g, after which, the probability of red-tagging fluctuates between 40% and 80%. This fluctuation is also seen in the probabilities of collapse for S_a values greater than 0.7g. The probability of red-tagging is driven by global collapse as well as by the collapse of the cripple walls, since very little damage is present in the structural components on the story above the cripple walls. Plots and details from the structural analysis results of the typical small house can be found in Porter et al. (2002).

A similar safety assessment procedure is taken for the *large house*, and the results of this analysis are given in Figure 10(b). This plot demonstrates that the *large house* performs better than the small house for low intensity levels. The large house has a near-zero probability of receiving a red tag resulting from a detailed evaluation for earthquakes with hazard levels less than or equal to S_a =0.8g. The probability of red tag increases linearly until S_a =1.3g; beyond this hazard level, the probability of red-tagging fluctuates between 60% and 80%. Unlike the small house, the large house does not have significant contributions to red-tagging from global collapse; most of the red tagging is caused by damage to the exterior shearwalls that is consistent with historical damage data from the Northridge Earthquake of single-family homes built in the same time period (Shierle 2003). The fluctuation in red-tagging for high levels of ground motion is also observed in the probabilities of the 'collapse' damage state for the exterior shearwalls (median of IDR, x_m = 1.1% and the logarithmic standard deviation of IDR, β = 0.5) in the first story. Again, plots and details from the structural analysis results of the typical *large house* can be found in Porter et al. (2002).

8 CONCLUSION

In this study, we explore the use of simplified structural models for use in rapid risk assessment of woodframe houses. Both simplified models perform equally well for the small house, and are able to accurately capture building collapse and the behavior of the cripple walls. It is reasonable to use either of these models for web-based risk modeling of one-story houses, especially if *EAL* is used as a performance metric. The *S1* model captures the damage and losses well of the large house but the, the *S2* model is unable to accurately depict the behavior of the exterior walls, which is where most of the damage is concentrated and thus resulting repair costs. Careful consideration should be taken with *S2* "like" models for risk assessment of multi-story residential buildings.

We have also shown the first steps for incorporating a comprehensive seismic virtual inspection methodology into the USGS interactive web-based tool, known as ResRisk-WH (Residential Risk – Woodframe Houses). This project explores a new MCS approach for the *virtual inspector*, and gives clear guidelines on how to build such a computational model, using building component fragility functions, for any type of structure. The damage and safety results of the

typical small house show that unbraced cripple walls in older single family homes are a safety hazard and reinforces the need for seismic mitigation of these types of walls. The results of the large house mimic those found in Shierle's (2003) field investigations after the Northridge earthquake. The fluctuations in tagging probabilities at high ground shaking intensity levels could be reduced with improved collapse analysis methods for woodframe structures.

The results of the virtual inspector stand on their own as essential information for building stakeholders. The results of this inspection, however, can be incorporated into building downtime modeling (Mitrani-Reiser and Beck 2007) and may used to estimate indirect losses associated with business interruption and delayed mobilization time prior to commencement of building repairs.

9 PUBLICATIONS/PRESENTATIONS RESULTING FROM THIS WORK

Mitrani-Reiser, J., Ryu, H., Luco, N., and Jones, N.P., 2009. "A Simplified Approach for Evaluating the Seismic Performance of Woodframe Houses," poster presented at the *Earthquake Engineering Research Institute Annual Meeting*, Salt Lake City, UT, February 2009.

Mitrani-Reiser, J., Luco, N., Ryu, H., and Jones, N.P., 2009. "Virtual Building Inspection for Open Risk Assessment Software," *Proc., 10th International Conference on Structural Safety and Reliability*, Osaka, Japan, September 2009.

Luco, N., Martinez, E.M., Field, E.H., Ryu, H., and Mitrani-Reiser, J., 2009. "An Interactive Web Tool for Quantitative Risk Assessment of Woodframe Houses ("ResRisk"): A Progress Report," *Proc., 10th International Conference on Structural Safety and Reliability*, Osaka, Japan, September 2009.

10 ACKNOWLEDGEMENT

The authors are thankful to their colleagues at the US Geological Survey, Dr. Nico Luco and Dr. Hyeuk Ryu for their collaboration on the structural modeling and their insightful feedback throughout the duration of the project. Additionally, support for this work was provided by the U.S. Geological Survey, Department of the Interior, under USGS Award No. 08HQGR0011. The views and conclusions contained in this document are those of the authors and should not be interpreted as necessarily representing the official policies, either expressed or implied, of the U.S. Government.

11 REFERENCES

Aslani, H. and Miranda, E., 2004. Component-Level and Sytem-Level Sensitivity Study for Earthquake Loss Estimation. Proceedings, Thirteenth World Conference on Earthquake Engineering. Vancouver, B.C., Canada.

(ATC) Applied Technology Council, ATC-20: Procedures for postearthquake safety evaluation of buildings. Redwood City, California, 1989.

(ATC) Applied Technology Council, ATC 20-2: Addendum to the ATC-20 postearthquake building safety evaluation procedures. Redwood City, California, 1995.

(ATC) Applied Technology Council, ATC 20-3: Case studies in rapid postearthquake safety evaluation of buildings. Redwood City, California, 1996.

Beck, J.L., Porter, K.A., Shaikhutdinov, R., Au, S.K., Moroi, T., Tsukada, Y., and Masuda, M., 2002. Impact of Seismic Risk on Lifetime Property Values, Final Report, Consortium of Universities for Research in Earthquake Engineering, Richmond, CA.

Carr, A.J., 2000. Ruaumoko - Inelastic Dynamic Analysis Program, Christchurch, New Zealand: Department of Civil Engineering, University of Canterbury.

(EERI) Earthquake Engineering Research Institute, 1996a. Wood Buildings, Chapter 6 in Supplement C to Volume 11 of Earthquake Spectra, Northridge Earthquake Reconnaissance Report, Vol. 2, 1996.

(EERI) Earthquake Engineering Research Institute, 1996b. Wood Buildings, Chapter 6 in Volume 11 of Earthquake Spectra, Northridge Earthquake Reconnaissance Report, 1996.

Goulet, C., Haselton, C., Mitrani-Reiser, J., Beck, J.L., Deierlein, G., Porter, K.A., Stewart, J.P.. and Taciroglu, E., 2007. "Evaluation of the Seismic Performance of a Code-Conforming Reinforced-Concrete Building - From Seismic Hazard to Loss Results," Earthquake Engineering and Structural Dynamics 36(13): pgs. 1973-1997.

Haselton, C.B., Goulet, C., Mitrani-Reiser, J., Beck, J.L., Deierlein, G.G., Porter, K.A., and E. Tacirtoglu, An assessment to benchmark the seismic performance of a code-conforming reinforced-concrete moment-frame building, PEER Report. University of California, Berkeley, California, in preparation, 2007.

Isoda, H., Folz, B., and Filiatrault, A., 2001. Seismic Modeling of Index Woodframe Buildings on Research Task 1.5.4., Consortium of Universities for Earthquake Engineering Research, Richmond, CA.

Mitrani-Reiser, J. An ounce of prevention: probabilistic loss estimation for perform-ance-based earthquake engineering, PhD Thesis in Applied Mechanics. California Insti-tute of Technology, Pasadena, California, 2007.

Mitrani-Reiser, J. and Beck, J.L., 2007. "Incorporating Losses Due to Repair Costs, Downtime and Fatalities in Probabilistic-Based Earthquake Engineering," Proc., Computational Methods in Structural Dynamics and Earthquake Engineering, Crete, Greece, June 2007.

Petersen, M.D., Frankel, A.D., Harmsen, S.C., Mueller, C.S., Haller, K.M., Wheeler, R.L., Wesson, R.L., Zeng, Y., Boyd, O.S., Perkins, D.M., Luco, N., Field, E.H., Wills, C.J., and Rukstales, K.S., 2008.

Documentation for the 2008 Update of the United States National Seismic Hazard Maps, U.S. Geological Survey Open-File Report 2008–1128, 61 pgs.

Porter, K. A., Beck, J. L., Seligson, H. A., Scawthorn, C. R., Tobin, L. T., Young, R., and Boyd, T., 2002. Improving Loss Estimation for Woodframe Buildings, Final Report, CUREE-Kajima Joint Research Program Phase IV, Consortium of Universities for Earthquake Engineering Research, Richmond, CA.

Schierle, G.G., 2003. Northridge Earthquake Field Investigations: Statistical Analysis of Woodframe Damage, Final Report, CUREE-Caltech Woodframe Project, Consortium of Universities for Earthquake Engineering Research, Richmond, CA.

Somerville, P., Smith, N., Punyamurthula, S., and Sun, S., 1997. Development of Ground Motion Time Histories for Phase 2 of the FEMA/SAC Steel Project, SAC Joint Venture, Background Document Report No. SAC/BD-97/04.

Stewart, W.G., 1987. "The Seismic Design of Plywood Sheathed Shear Walls," Ph.D Report, Department of Civil Engineering, University of Canterbury, New Zealand.